Department of Applied Mathematics
Faculty of EEMCS

University of Twente
The Netherlands

P.O. Box 217
7500 AE Enschede
The Netherlands
Phone: +31-53-4893400
Fax: +31-53-4893114
Email: memo@math.utwente.nl
www.math.utwente.nl/publications

Memorandum No. 1788

Reservoir formation in shallow granular flows through a contraction

M. Al-Tarazi[1], O. Bokhove, J.A.M. Kuipers[1],
M. van Sint Annaland[1] and A.W. Vreman[2]

December, 2005

ISSN 0169-2690

[1]Department of Chemical Engineering, University of Twente, Enschede, The Netherlands
[2]Vreman Research, Hengelo, The Netherlands

Reservoir formation in shallow granular flows through a contraction

M. Al-Tarazi[1], O. Bokhove[2], J.A.M. Kuipers[1], M. van Sint Annaland[1]
University of Twente, Enschede, The Netherlands
[1] *Department of Chemical Engineering;* [2] *Department of Applied Mathematics* *

A.W. Vreman
Vreman Research, Hengelo, The Netherlands
(Dated: December 20, 2005)

We consider flow of dry granular matter down an inclined chute with a localized contraction. Measurements and analysis show that changes in particle volume fraction are important, especially across granular bores. For fixed upstream conditions and depending on the nozzle width of the contraction, we observe either small oblique jumps, a reservoir with a steady jump, or a reservoir with an upstream traveling bore. Shallow layer theory extended to include porosity changes qualitatively predicts these regimes. Implications for volcanic debris flows are discussed.

PACS numbers: - *AMS* numbers: 82D99 86A60 74A30 *Keywords:* granular flow and hydraulics, experiments

Understanding of the hydrodynamics of the flow of granular matter such as sand, pills and dry food particulates would greatly aid in the design and control of materials handling equipment. In contrast to "classical" fluid dynamics, the governing constitutive equations describing the dynamics of granular materials are not well-known. Several approaches are attempted, often in unison, to predict and understand granular dynamics. These include: discrete particle mechanics [1]; (simplified) continuum theories based on kinetic theory of granular particles [2]; and, asymptotic models [3]. In the following geological example the Rhine River is the carrier fluid with tephra as floating and submerged granular material. During the late Pleistocene (12.900 aBP), the Laacher See Volcano in the Eifel region of Germany violently exploded, and is estimated to have led to an initial 1–8 m layer of tephra around the volcano [4]. There is evidence that this tephra layer caused dam formation in the Rhine River at a nozzle in the valley near Andernach. A large lake formed extending 50 km to the southeast. The dam subsequently collapsed. Can we make a theory and corresponding laboratory experiment in support of this event? The added complexity of a carrier fluid led us to consider a simpler question first: what flow regimes emerge when dry gravity-driven granular matter flows down an inclined chute with a contraction? We show that the following flow regimes qualitatively agree with predictions by shallow layer theory: I) steady supercritical flow with small-amplitude oblique granular jumps; II) steady flow with a reservoir formed by a large-amplitude jump in the contraction; and, III) flow with a reservoir in the entire contraction until an upstream traveling granular bore.

The flow of dry granular material is considered moving under gravity from an upstream supply through an aluminum chute inclined under an angle θ, see Fig. 1. The bottom of the chute is smooth, flat, 0.13 m wide and 2 m long. Spherical glass beads are used with diameter $d = 0.5$–$0.6\,mm$ and particle density $\rho_d = 2500\,kg/m^3$. The flow is regulated by an inlet slit of set thickness and a continued supply of particles from a tank. The shallow flow develops $\sim 0.2\,m$ downstream to a thickness smaller than the inlet thickness of 4 mm. We define the coordinate down along the chute as x, the one normal to the chute as z, and y as the direction across; t is time. With g the gravitational acceleration, its components normal to and along the chute are $g_n = g\cos\theta$ and $g_t = g\sin\theta$.

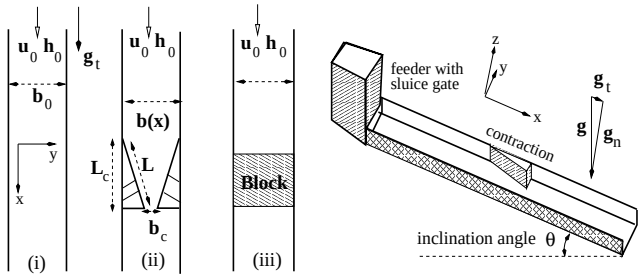

FIG. 1: Top and side view sketches of the inclined chute experiments: (i) of constant width, $b(x) = b_0$; (ii) with a localized contraction; and, (iii) blocked in the middle, "$b_c = 0$".

Pouliquen [5] summarizes and extends many chute flow experiments, and distinguishes flows on smooth, intermediate and rough inclined planes. Steady uniform flows can be observed when the angle of inclination θ lies around the basal friction angle ϕ. For $\theta \gg \phi$ the flow accelerates. We limit ourselves to flows for which $\theta \approx \phi$, in which the gravitational force along the chute approximately balances the frictional forces.

Three types of experiments are performed: (i) uniform flow on a plane chute of constant width, $b(x) = b_c^* = b_0$; (ii) steady flow through a contraction linearly decreasing to width b_c^* at a nozzle, and (iii) granular bore formation for blocked flow, "$b_c = 0$", see Fig. 1.

Experiments. (i) Consider granular flow in a chute of

*Corresponding author: Dr. Onno Bokhove; Department of Applied Mathematics, University of Twente, P.O. Box 217, Enschede, The Netherlands; o.bokhove@math.utwente.nl

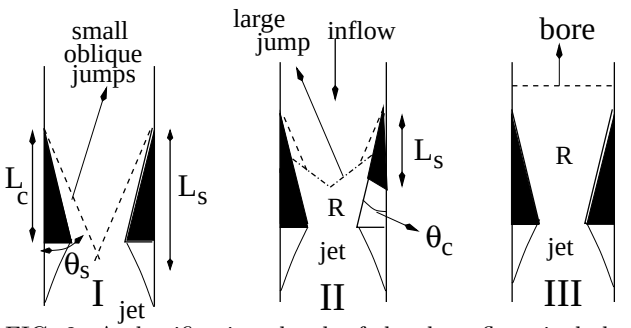

FIG. 2: A classification sketch of the three flows include: I) steady supercritical flow, $b_c^* \lesssim b_0$; II) steady flow with a reservoir, denoted by "R"; and, III) flow with reservoir and an upstream traveling bore, $b_c \gtrsim 0$. All cases have a jet behind the contraction. Dashed(-dotted) lines are jump or bore fronts.

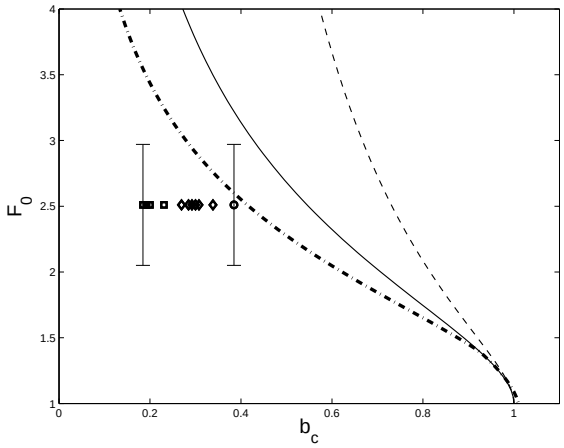

FIG. 3: Flow regimes arising from data and one-dimensional shallow layer theory are denoted in the parameter plane spanned by F_0 and b_c. *Data:* for one fixed $F_0 = 2.51 \pm 0.46$ (error bar), we observe: I) oblique jumps (square); II) a steady reservoir with a big jump (diamonds); and, III) a reservoir with upstream moving bore (triangles). *Incompressible theory:* The thin solid curve divides supercritical smooth flows (regime I), to the right, from nonsmooth flows, to the left. The thin dashed curve divides a reservoir with upstream moving bore (regime III) from smooth supercritical flow. The above two regimes exist between the dashed and solid curves and an unstable reservoir with steady jump (regime II). *Compressible theory:* A prescribed, but experimentally partly constrained, variation of the volume fraction leads to a leftward shift of the solid to the thick dashed-dotted curve (arrow).

constant width and inclination θ=15.5^o. We have measured the average velocity and the velocity on top of the granular layer with Particle Image Velocimetry (PIV). Except for an inflow region, the flow has nearly constant velocity along and across the chute with a thickness of $(2.34 \pm 0.07)\,mm$. The average velocity is inferred by measuring the mass flux at the end of the chute, the layer thickness h, the particle density, the width b_0, and the particle volume fraction with a trapping method [5], giving $\alpha = 0.36 \pm 0.06$. The average velocity and PIV velocity are $(0.37 \pm 0.07)\,m/s$ and $(0.46 \pm 0.01)\,m/s$. Since the velocity of the top layer is higher than the average velocity, [6], we use a Froude number $F_0 = 2.51 \pm 0.46$ based on this average velocity.

(ii) After this assessment of the inflow conditions, we consider the flow through a contraction linearly decreasing from $b_0 = 0.13\,m$ to the nozzle value b_c^*. Thereafter $b(x) = b_0$. See Fig. 1(ii). By using the same inflow with $F_0 = 2.51 \pm 0.46$, we explore flows by varying $b_c = b_c^*/b_0$. Three flow regimes are observed, see Fig. 2: I) for $b_c \geq 0.38$ ($b_c^* \geq 5.0\,cm$) supercritical flows occur in which the small-amplitude oblique jumps may cross (square in Fig. 3); II) for $0.27 < b_c < 0.38$ ($3.5\,cm < b_c^* < 5.0\,cm$) a stable slow-flowing and low-porosity reservoir forms upstream of the nozzle with a large curved granular jump or "Mach stem" adjusting to the upstream conditions (diamonds in Fig. 3); and III) for $b_c < 0.27$ a stable reservoir forms with an upstream traveling granular bore (triangles in Fig. 3). At $b_c = 0.27$, the nearly straight bore front at the side wall matches the beginning of the contraction. A snapshot of the flow (PIV) for the steady reservoir case in Fig. 4 shows that the small oblique granular jumps run into a large jump. Measurements with only one half of the obstruction confirm that the amplitude across the oblique jumps is smaller than across the jump in the reservoir. The thickness h and volume fraction α versus x are given in Fig. 5 for $b_c^* = 2.0, 2.6, 4.4, 5.0\,cm$ with fixed $F_0 = 2.51 \pm 0.46$. Cases with $b_c^* = 2.0, 2.6\,cm$ have an upstream moving bore which has halted, see Fig. 5, against the flow coming out of the feeding tank. In all cases, a jet exits the nozzle with a free boundary demarcating the particle-free regions. In Fig. 5, the thickness in the jet region is seen to decline from the reservoir to the background values.

Theoretical predictions. The variations of flow properties normal to and across the chute are smaller than the ones along the chute, since the flow depth is shallow and the chute narrow. This has led to equations akin to the shallow water equations, but with more complicated frictional terms (e.g., [3]). We therefore try to predict the experimental flow behavior based on leading-order shallow layer theory. We arrive at continuity and momentum equations for averaged quantities by asymptotic analysis of the Lun et al. [2] equations. We derive hydrostatic balance in the z-direction, $\partial M/\partial z = -\tilde{\alpha}\, g_n$, with granular pressure $\rho_d\, M$ and particle volume fraction $\tilde{\alpha}(x, y, z, t)$, and then average the equations of motion across z and integrate $\partial M/\partial z = -\tilde{\alpha}\, g_n$ using that $\tilde{\alpha} \approx \alpha(x, y, t)$. See [3] for the case with $\tilde{\alpha}$ constant. Fluctuations are ignored. The dimensionless depth-averaged equations are

$$\begin{aligned} &\partial_t(\alpha\, h) + \partial_x(\alpha\, h\, u) + \partial_y(\alpha\, h\, v) = 0 \\ &\partial_t(\alpha\, h\, u) + \partial_x\big(\alpha\, h\, u^2 + \frac{\alpha\, h^2}{2\, F_0^2}\big) + \partial_y(\alpha\, h\, u\, v) = 0 \\ &\partial_t(\alpha\, h\, v) + \partial_x(\alpha\, h\, u\, v) + \partial_y\big(\alpha\, h\, v^2 + \frac{\alpha\, h^2}{2\, F_0^2}\big) = 0, \end{aligned} \qquad (1)$$

where we defined depth $h(x, y, t)$, depth-averaged planar velocity $\mathbf{v}(x, y, t) = (u, v)^T$ and particle volume fraction

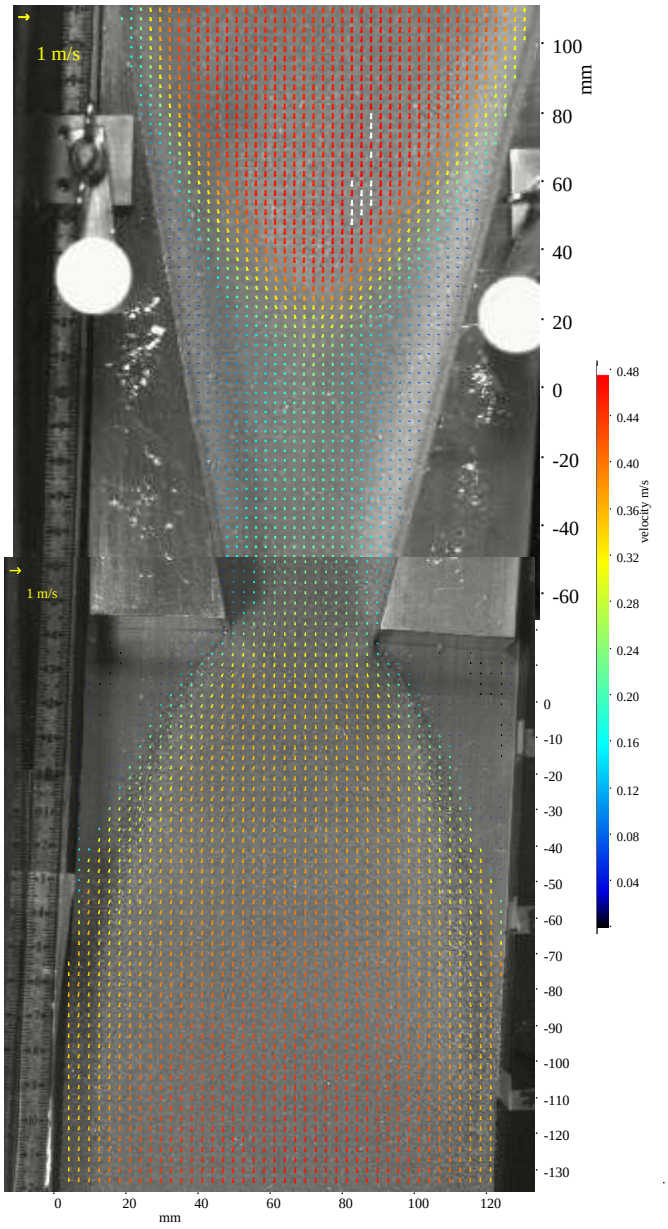

FIG. 4: A snapshot is shown of the granular flow in case of a steady reservoir with $b_c^* = 4.4\,cm$.

$\alpha(x, y, t)$. No friction is included since for inclinations with $\theta \approx \phi$ and fast flows the frictional terms cancel to leading order against the gravitational force, and we also used $v \ll u$. We scaled Eqs. (1) using $x^* = b_0\,x$, $(u^*, v^*) = u_0\,(u, v)$, $t^* = (b_0/u_0)\,t$, $h^* = h_0\,h$ and defined a Froude number $F_0 = u_0/\sqrt{g_n\,h_0}$, all based on the uniform upstream values b_0, h_0, u_0 (dimensional variables are denoted with asterisks).

For fast steady flows oblique granular jumps emerge at the beginning of the contraction. We define the angle θ_c of the wall of the contraction and the angle $\theta_s > \theta_c$ of the oblique jumps, relative to the parallel wall of the chute, see Fig. 2. When the oblique jumps exist, the angle θ_s

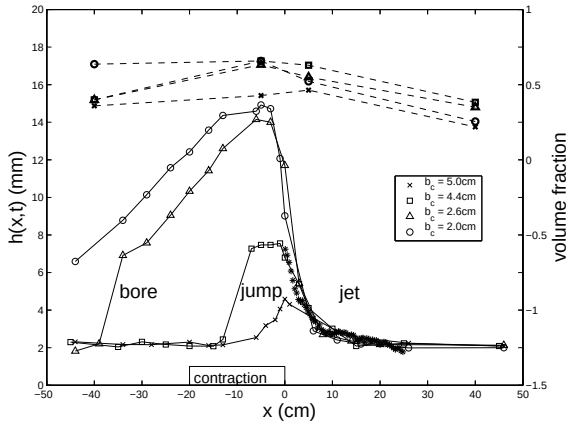

FIG. 5: With $F_0 = 2.51 \pm 0.46$ and $\theta = 15.5^o$, the measured layer thickness (solid lines) and volume fraction (dashed lines) versus x are shown for various b_c's: $b_c^* = 5.0\,cm$, nearly smooth supercritical flow; $b_c^* = 4.4\,cm$, a reservoir with steady granular jump; and, $b_c^* = 2.0$, and $2.6\,cm$, a reservoir with upstream moving granular bore. The stars for case $b_c^* = 4.4\,cm$ correspond to discrete hard-sphere particle simulations starting at the nozzle. Volume fraction is measured by trapping particles in a cup [5].

follows from the bore relations for Eqs. (1) (see [7]):

$$\sin\theta_s = \sqrt{\frac{1}{2\,F_0^2}\,\frac{\alpha_+\,h_+}{\alpha_0\,h_0}\,\frac{1-\alpha_+\,h_+^2/(\alpha_0\,h_0^2)}{1-\alpha_+\,h_+/(\alpha_0\,h_0)}}, \qquad (2)$$

where α_+, h_+ are the constant values downstream of the jump. The direction of the flow $\mathbf{v}_+$ is along the wall of the contraction, which length $L = 0.198\,m$ is fixed. For constant porosity, $1-\alpha$, Eq. (2) reduces to Eq. (4.2) in [3]. Using conservation of mass in a control volume situated around the point of inclination, we derive ([7])

$$\alpha_+\,h_+/\alpha_0\,h_0 = \tan\theta_s/\tan(\theta_s - \theta_c). \qquad (3)$$

Combining the two we obtain θ_s as function of F_0 for given θ_c. For each θ_c and thus b_c, there exist a minimum F_0 for which such (multiple and crossing) oblique jump solutions exist, [7]. For smaller Froude numbers, the shallow layer analogy of a Mach stem will appear, [7], as suggested in Fig. 4. However, we do not know the relation between porosity and the other flow variables, or the granular temperature. We therefore consider a one-dimensional theory by averaging (1) across the width of the contraction, thus eliminating any explicit y-dependence, to obtain

$$\begin{aligned} \partial_t(\alpha\,h\,b) + \partial_x(\alpha\,h\,b\,u) &= 0 \\ \partial_t(\alpha\,h\,b) + \partial_x\big(\alpha\,h\,b\,u^2 + \frac{1}{2}\,\alpha\,b\,\frac{h^2}{F_0^2}\big) &= \frac{1}{2}\,\alpha\,\frac{h^2}{F_0^2}\,\partial_x b. \end{aligned} \qquad (4)$$

First, we solve (4) in steady state for constant α, cf. [8]. The associated smooth solutions only exist to the right of the limiting curve $b_c = \big(3/(2+F_0^2)\big)^{3/2}\,F_0$, denoted by the solid line in Fig. 3, and defined by imposing criticality, $F = u\,F_0/\sqrt{h} = 1$, at the nozzle. Upstream moving bores occur to the left of the dashed line, and three

states exist between the solid and dashed line: upstream moving bores; smooth supercritical flow; and, a steady jump in the contraction [8]. Without friction this steady jump is unstable. Due to friction it is marginally stable in horizontal flume experiments with water, which shifts the thin curves to the right [8]. In contrast, our steady granular reservoir is stable and emerges as the preferred state, while our experimental data lie to the left of the solid and dashed curves based on incompressible shallow flow. This anomaly is explained below.

In experiment (iii) in Fig. 1, "$b_c = 0$" as the flow is blocked and thus resembles the upstream moving bore case III. Consider a constant upstream state with u_0, h_0, α_0; and a quiescent state with $u_+ = 0, h_+, \alpha_+$ downstream of the bore. The jump relations for Eqs. (1), cf. [7], yield the bore speed in dimensional form

$$S_\alpha = -\sqrt{\frac{g_n}{2}\,\frac{\alpha_0\,h_0}{\alpha_+\,h_+}\,\frac{(\alpha_+\,h_+^2 - \alpha_0\,h_0^2)}{(\alpha_+\,h_+ - \alpha_0\,h_0)}}. \qquad (5)$$

Given h_0, α_0, h_+ and α_+ we can predict S_α and u_0. For constant α, Eq. (5) reduces to the granular bore speed $S = \lim_{\alpha_0=\alpha_+} S_\alpha$ used by [3]. We measured the bore speed using PIV , and calculated it using Eq. (5) employing: measured thicknesses $h_{0,+}$; upstream particle volume fraction $\alpha_0 = 0.36 \pm 0.06$; and, downstream maximum packing $\alpha_+ = 0.65$ (see Fig. 5). The calculated and measured bore speeds are $S_{meas} = 0.073\,m/s$, $S = 0.11\,m/s$ and $S_\alpha = (0.078 \pm 0.008)m/s$, differing 34 % with the standard bore speed S for constant porosity, and $[4, 14]$% with the new bore speed S_α. This further confirms that θ=15.5^o lies close to the basal friction angle ϕ.

Experiment (iii) thus indicates that porosity matters. We therefore repeat the one-dimensional calculation for varying volume fraction by using:

$$\alpha = \alpha_0^- + (\alpha_+ - \alpha_0^-)\,(F_0 - F)/F_0 \qquad (6)$$

with $\alpha_0^- = \min(\alpha_+, \alpha_0\,F_{03}/F_0)$. A dependence on Froude number seems reasonable as $\alpha = \alpha_+$ when $F = 0$ and $\alpha = \alpha_0 = 0.36$ when $F = F_0 = F_{03} \approx 2.51$. For $F = F_0 > F_{03}$ we expect more aerated flow so that α decreases. Including this porosity dependence on F in (6) into the one-dimensional steady state theory, leads to a shift of the solid curve based on $\alpha = cst.$ to the dashed-dotted curve in Fig. 3. Hence, even our simple, imposed relationship between volume fraction and Froude number result in a closer agreement with the observations. Somewhat heuristically, we could also include the α-dependence only in the continuity equation and define an effective width $\tilde{b} = \alpha\,b$, potentially larger than b_0. The dashed and solid curves in Fig. 3 then also shift to the left as α increases. Increase of α can possibly lead to a local widening of the effective "contraction" width, which is known to stabilize the steady jump in the contraction [8].

In conclusion, the three observed flow regimes correspond qualitatively with the ones suggested by an extended shallow layer theory. The quantitative differences between theory and experiment occur because porosity changes are shown to matter for the fast flows with $h/d < 10$, shown here and in [3], while such flows with $h/d \approx 20$ may be more incompressible [9]. Standard shallow layer bore theory can likely be improved by including the (observed) porosity jumps even though it is presently unclear how to predict porosity, and a phenomenological velocity- and depth-dependent friction law for the granular material [6]. Preliminary simulations with a hard-sphere discrete particle model [1] predict the jet behind the contraction well, see Fig. 5.

Finally, reservoir formation in our experiment was caused by granular hydraulics and not by dam formation, as in Schmincke's hypothesis [4] on lake formation after the Laacher See Volcano eruption. The dynamics of the tephra and water mixture in that case was, however, more complex and slower.

Acknowledgments

O.B., M.A. and A.W.V. acknowledge support via the Royal Netherlands Academy of Arts and Sciences, and the Institute for Mechanics, Processes and Control - Twente. O.B. thanks: Prof. H.-U. Schmincke for his guidance in the Eifel; Profs. C. Connor and D.H. Peregrine, and the participants in the GFD Fellowship program 2005 of the Woods Hole Oceanographic Institution for their valuable remarks.

[1] B.P.B. Hoomans, J.A.M. Kuipers, W.J. Briels, & W.P.M. van Swaaij, 'Discrete particle simulation of bubble and slug formation in a two-dimensional gas-fluidized bed: a hard-sphere approach'. *Chem. Engng. Sci.* **51**, 99–118 (1996).

[2] C.K.K. Lun, S.B. Savage, D.J. Jeffrey, & N. Chepurniy, 'Kinetic theories for granular flow: inelastic particles in Couette flow and slightly inelastic particles in a general flowfield'. *J. Fluid Mech.* **140**, 223–256 (1984).

[3] J.M.N.T. Gray, Y.-C. Tai, & S. Noelle, 'Shock waves, dead zones and particle-free regions in rapid granular free-surface flows'. *J. Fluid Mech.* **491**, 161–181 (2003).

[4] H.-U. Schmincke, *Vulkanismus.* Wissenschaftiche Buchgesellschaft Darmstadt, 264 pp. (2000).

[5] O. Pouliquen, 'Scaling laws in granular flows down a rough inclined plane'. *Physics of fluids* **11**, 542–548 (1999).

[6] GDR MiDi, 'On dense granular flows' *Eur. Phys. J. E* **14**, 341–365 (2004).

[7] A.H. Shapiro *The dynamics and thermodynamics of compressible fluid flow.* New York. 647 pp. Chps. 5 & 16.

[8] Flow over a hill: P.G. Baines & J.A. Whitehead, 'On multiple states in single-layer flows'. *Phys. Fluids* **15**, 298–307 (2003); and: B. Akers 'Shallow water flow through a contraction'. Report Geophysical Fluid Dynamics Fellowship Program, Woods Hole Oceanographic Institution (2005).

[9] K.M. Hákonardóttir and A.J. Hogg, 'Oblique shocks in rapid granular flows'. *Phys. Fluids.* **17**, 077101 (2005).